
SPIKING NEURAL PREDICTIVE CODING FOR CONTINUAL LEARNING FROM DATA STREAMS

Alexander Ororbia

Department of Computer Science
Rochester Institute of Technology
Rochester, NY 14623
ago@cs.rit.edu

ABSTRACT

For energy-efficient computation in specialized neuromorphic hardware, we present the Spiking Neural Coding Network, an instantiation of a family of artificial neural models strongly motivated by the theory of predictive coding. The model, in essence, works by operating in a never-ending process of “guess-and-check”, where neurons predict the activity values of one another and then immediately adjust their own activities to make better future predictions. The interactive, iterative nature of our neural system fits well into the continuous time formulation of data sensory stream prediction and, as we show, the model’s structure yields a simple, local synaptic update rule, which could be used to complement or replace online spike-timing dependent plasticity. In this article, we experiment with an instantiation of our model that consists of leaky integrate-and-fire units. However, the general framework within which our model is situated can naturally incorporate more complex, formal neurons such as the Hodgkin-Huxley model. Our experimental results in pattern recognition demonstrate the potential of the proposed model when binary spike trains are the primary paradigm for inter-neuron communication. Notably, our model is competitive in terms of classification performance, can conduct online semi-supervised learning, naturally experiences less forgetting when learning from a sequence of tasks, and is more computationally economical and biologically-plausible than popular artificial neural networks.

Keywords Spiking neural networks · online learning · continual learning · semi-supervised learning · data streams

1 Introduction

Through the extraction of rich, expressive hierarchies of feature detectors from large samples of patterns, artificial neural networks (ANNs) have become popular, powerful models of data. ANNs continue to demonstrate their powerful function approximation abilities in an ever-growing variety of applications [48, 82, 87, 84], including many in computer vision [51, 38], speech [40, 69], and text processing [80, 18, 76]. However, despite these recent successes, ANNs, in their current form, face some significant difficulties. These range from problems in effective implementation in (neuromorphic) hardware meant for real-time computation [10, 45] to challenges in parameter optimization [83] to designing agents that generalize well across tasks and datasets [96, 101]. The source of many of these issues might result from the fact that ANNs are only very loosely inspired by the brain. In essence, artificial neurons lack many of the actual mechanisms that underlie the real biological neurons that, when taken en masse, give rise to the complex cognitive functioning and behavior that is characteristic of human agents. If the hope is to one day build neural systems that better exhibit such behavior, one direction that might prove fruitful would be to bridge the gap between artificial and real neurons. Recently, a line of ANN research has begun to more deeply investigate this hypothesis, focusing on formalizing and implementing various types of neural computation and learning mechanisms currently known in cognitive neuroscience. This brand of connectionism, also known as biologically- or neurocognitively-plausible learning, has already begun to show that by modeling and integrating neurobiological mechanisms, e.g., lateral inhibition [34, 68, 1, 93, 52, 73], neurotransmission [60, 22, 2], local weight update rules [47, 77, 75], we might be either able to generalize differently or, at the very least, side-step some of the issues related to classical ANN learning algorithms, i.e., back-propagation of errors (backprop) [32]. This body of work continues to slowly provide evidence that by more

faithfully modeling how real neurons compute and conduct credit assignment, we might develop agents capable of recognizing and processing complex patterns in noisy environments.

One of the key differences between the neurons in ANNs and actual neurons is in how information is communicated across the individual units of the system. ANN neurons communicate with continuously graded values, typically requiring activation/transfer functions that are differentiable. In contrast, inter-neuron communication in real-world neurons is performed through the broadcasting of action potentials, creating what is known as spike trains [17]. These series of spikes are sparse in time, yet each spike carries a great deal of information. This serves as one primary inspiration for the spiking neural network (SNN) model, often used in computational neuroscience, which encodes sensory information content through the precise timing of spikes [56]. The sparse, spike-based communication inherent to SNNs is, in fact, one of their primary strengths. ANNs require the use of energy-intensive, top-of-the-line graphics processing units (GPUs) for effective training while SNNs consume dramatically less energy through the use of high-information content spike trains, facilitating the construction of very fast, energy-efficient hardware to support their processing, i.e., neuromorphic hardware [30, 62, 16]. Importantly, the low energy-consumption, hardware-friendly nature of SNNs make them ideally suited for use in pattern processing and adaptation in complex real-time systems, such as robotic agents [35, 90] or self-driving cars [44].

However, despite their potential, SNN research and simulation is still in its early stages (in contrast to second-generation ANNs) where the adjustment of the synaptic weights that connect the internal neurons poses one of the greatest (open) challenges. Since the spike trains of an SNN are formally represented as summations of Dirac delta functions, differentiation no longer applies, quickly ruling out the use of backprop.¹ One common, biologically-plausible (Hebbian) rule used to adjust SNN synapses is spike-timing dependent plasticity (STDP) [8], which takes into account the temporal ordering of spikes in order to conduct either long-term potentiation (LTP), where a weight strength is increased, or long-term depression (LTD), where a weight strength is decreased. However, STDP is typically applied over a temporal window, similar in spirit to backprop through time (BPTT) [97], making it ill-suited to incremental, real-time learning, something that the human brain is clearly able to do. Though STDP can be formulated to operate online, real-time, online adjustment of SNN weights remains an extremely difficult challenge, and, in the case of SNNs with more than one layer, STDP and related approaches often struggle to incrementally train the model properly.

In order to tackle the difficult problem of effectively and efficiently learning multiple layers of spiking neurons, we will start by first reformulating the SNN architecture under the *spiking neural coding* framework, which aims to bridge the recently proposed discrepancy reduction family of learning algorithms [74] with core computational principles of networks of spiking neurons [56, 25]. Discrepancy reduction algorithms are fundamentally motivated by the neuro-mechanistic theories of predictive coding [29, 4, 88], prospective coding [86, 50], and analysis by synthesis [66]. The central idea behind predictive coding is that the brain could be viewed as a top-down, directed generative model that first actively generates hypotheses (or predictions) and then immediately corrects itself in the presence of environmental stimuli. In the statistical learning literature, this theoretical framework has been concretely implemented and extended to include how weight adjustment is conducted locally, recently branded as neural predictive coding (NPC) [73]². One of the primary contributions of this work is to recast the core principle components and ideas behind SNNs into the framework of NPC. Unlike most current SNNs, which are designed to operate like typical feedforward or recurrent ANNs, we will show that the iterative nature of NPC is naturally suited to continuous-time presentation of input stimuli, allowing it to perform continual error-correction [72] in order to build up dynamic distributed representations of data from spike trains. Furthermore, by doing so, the NPC-formulated SNN can easily exploit a simple, neurocognitively-plausible, coordinated local learning rule known as local representation alignment, which could be used in place of or in tandem with STDP.

2 Continual Error-Correction from Spike Trains

2.1 Problem Definition: Continually Predicting Sensory Stream Inputs

In this article, the neural agents we are ultimately concerned process sensory stimuli, which are sampled from an environment or a stochastic process over time. The patterns presented to the neural system are to be viewed as a continuum, i.e., $\{(y_1, \mathbf{x}_1) \dots (y_n, \mathbf{x}_n)\}$ with n examples, though in the case of most real-world application streams, there would be no finite bound on the number of samples. At any particular instant, \mathbf{x}_j represents the feature vector of the j^{th} example and y_j is the target (or, in the case of auto-association or autoencoding, $y_j = \mathbf{x}_j$). Note that the

¹Though there is no lack of effort in attempting to manipulate backprop to work with SNNs [12, 54]. Other efforts often attempt to convert backprop-trained ANNs to non-trained equivalent SNN models [21].

²This naming has been used to distinguish it from the classical signal processing usage of the phrase “predictive coding” [3], which has also seen recent integration into SNN learning and inference [11].

agent will process any instance only once as it continues through the sample stream, meaning that no exact data point previously seen can be retrieved for additional repeated processing as is typically done when training most ANNs. The main task for any learner receiving samples from such a continuum is to extract as quickly as possible enough information about the (nonstationary) distribution that governs the observations received in order to effectively predict the target y_j for any given x_j . Other tasks are possible, e.g., the learner could ideally learn how to reconstruct/generate x_j over a finite time horizon which characteristic of the generative modeling of a time-series and would be useful in supporting higher-level cognitive activities such as planning in robotics.

The data stream formulation presented here still treats each data point as a discrete element although SNNs are intended to process input stimuli that arrive within the flow of continuous time. In order to truly adapt the above stream to SNNs, we must also note that each tuple (y_j, x_j) is presented to the learner for a fixed period of simulated time. More importantly, this vectors in this tuple are mapped to an appropriate spike train encoding, i.e., a Poisson spike train. In essence, a tuple is to be presented to the agent for a specified stimulus interval of T_{st} milliseconds (ms), optionally followed by an inter-stimulus time of T_{ist} ms. The length of the stimulus and inter-stimulus times will vary depending on the data problem and application, e.g., frames of a video might be presented for a shorter stimulus interval (30 – 50 ms) while static images might be presented for a longer period (100-200 ms).

2.2 The Spiking Neural Coding Network

Next, we present a mechanistic description of our proposed spiking neural coding framework for handling the continuous-time data prediction problem above. In principle, the spiking neural coding network (SpNCN), the model instantiation of our framework, could be designed to work with any type of simulated neuron, including complex, more biologically-faithful ones, e.g., Hodgkin–Huxley [42] or Izhikevich [46] neurons. However, we will formulate the system using the leaky integrate-and-fire (LIF) neuron, one of the simplest spiking unit models. Though it ignores most biophysical details of the act of spiking, the LIF model is computationally cheaper to simulate and captures the core intuition behind how neurons behave in the presence of input [71, 24]. In the LIF, the rate at which spikes are produced is positively correlated with the strength of the current that enters a cell.³

In order to ease the mapping of the general structure underlying the previously proposed variations of the neural coding network (NCN) to the continuous spike-timing domain, we will develop the important model equations for inference and learning in matrix-vector form. We start from a neuronal unit-agnostic form of the SpNCN – meaning that any type of potentially complex neuronal unit, i.e., Hodgkin-Huxley units, could be integrated and used – before specifying the exact specification of the LIF variant we experiment with in this work. As is the case with determining the exact specification of abstract NPC-based models used in standard machine learning literature [73] (which work similarly to rate-coded models), the general NCN can be defined in terms of three key computations: 1) prediction or hypothesis generation, 2) error-correction, and 3) weight adaptation. From the perspective of spike-trains, the first two computations can be described in terms of how they affect the input current $\mathbf{J}^\ell(t)$ that is fed to a block of cells (at layer ℓ). Consider the case of an SpNCN with L layers of cells (one layer of sensory/actuary cells, $L - 1$ layers of internal processors), where we specify the (binary) spike vectors for any layer as $\mathbf{s}^\ell(t)$ and their filtered transformations as $\mathbf{z}^\ell(t)$. The spike vectors are produced by some spike-response model (SRM) $(\mathbf{v}^\ell(t), \mathbf{s}^\ell(t)) \leftarrow f_{srM}(\mathbf{v}^\ell(t), \mathbf{J}^\ell(t))$, which is a function that takes in an input current and the state of the voltage variable block we are interested in tracking. The SRM, which we will leave unspecified for now, captures the essence of most neuronal behaviors one would like to model given the limit of computational resources available for simulation. To compute the filtered transform of a binary spike vector \mathbf{s}_t^ℓ , we make use of a simple low-pass filter or variable trace defined as follows:

$$\mathbf{z}^\ell(t) = (1 - \alpha_f)\mathbf{z}^\ell(t) + \alpha_f\mathbf{s}^\ell(t), \quad \text{or,} \quad \mathbf{z}^\ell(t) = (\alpha_f\mathbf{z}^\ell(t)) \otimes (1 - \mathbf{s}^\ell(t)) + \mathbf{s}^\ell(t) \quad (1)$$

which only incurs the cost of extra memory needed to track layer ℓ 's last filtered output state. Note that \otimes denotes the Hadamard product and α_f is an interpolation constant, normally a function of the user-defined variable τ_f , where $\alpha_f = \exp(-\frac{\Delta t}{\tau_f})$. The second form of the filter in Equation 1 (the trace) functions as a bounded decaying memory used often in implementations of online STDP. Importantly, using a low-pass or trace filter allows us to smooth out the sparse spike trains generated by the raw SRM while still being biologically-plausible, and functions similarly to a rate-coded equivalent value that is maintained by the actual neuronal cells, possibly in the form of the concentration of internal calcium ions [71].

In order to compute the input currents needed for an SRM, we must first specify the first two computations of the NCN. Starting from the spike variable blocks $\{\mathbf{s}_t^1, \mathbf{s}_t^2\}$, which are output from the underlying SRMs, the NCN makes local

³Note that we are furthermore simulating point approximations of neural cells, which exploit the fact that the electrical signals that propagate from the dendrites to the cell body are essentially averaged together [71].

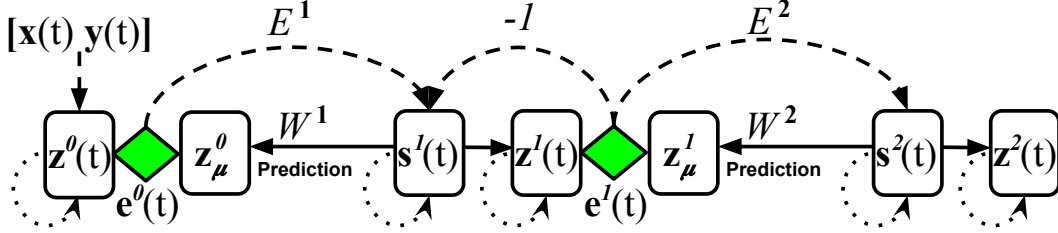


Figure 1: A 2-layer spiking neural coding network architecture. Green diamonds indicate error units ($e^0(t)$, $e^1(t)$), which, in this model, compute the amount of mismatch between the current predictions (z_μ^0 , z_μ^1) and the target signal traces ($z^0(t)$, $z^1(t)$). Variables $s^0(t)$, $s^1(t)$ represent the binary spikes (or output of the underlying spike response model) of a particular vector grouping of neuronal units at time t . Dotted arrows represent recurrent transmission of the last known value of the relevant variable. Mismatch signals are carried back across sets of synaptic weights (a mixture of excitatory and inhibitory connections) and used to adjust the current action potential of various spiking neurons.

predictions, in parallel, as follows:

$$z_\mu^\ell = W^\ell \cdot s^\ell(t), \quad e^\ell(t) = (z_\mu^\ell - z^\ell(t)) \quad (2)$$

where the (predictive) synaptic weights for a layer ℓ are organized into a matrix W^ℓ . Note that \cdot denotes a matrix multiplication. Mismatches between these predictions and currently-existing filtered state variables are then computed by an additional, coupled set of error neurons $e^\ell(t)$, as depicted in the equation above. In the brain, our claim is that, much in the same vein as [29], error neurons (and the error weights) can be related to superficial pyramidal cells which pass along mismatches signals while deep pyramidal cells pass along predictions from state units.⁴ These error neurons, the key to the inherent continual error-correction process of the NCN and predictive coding theories in general, are now to be treated in continuous-time as well. When these error cells are connected recurrently to neurons in a nearby layer, introducing two new additional sets of synaptic weights $\{E^1, E^2\}$ (or error synapses), we may compute the input current to each layer as follows:

$$\mathbf{J}^\ell(t) = (1 - \kappa)\mathbf{J}^\ell(t) + \kappa \left(-\gamma_J \mathbf{J}^\ell(t) + \phi(-e^\ell(t) + E^\ell \cdot e^{\ell-1}(t)) \right) \quad (\text{Intermediate layer}) \quad (3)$$

$$\mathbf{J}^L(t) = (1 - \kappa)\mathbf{J}^L(t) + \kappa \left(-\gamma_J \mathbf{J}^L(t) + \phi(E^L \cdot e^{L-1}(t)) \right) \quad (\text{Topmost layer}) \quad (4)$$

where $\kappa = \exp(-\frac{\Delta t}{\tau_J})$ (τ_J is the synaptic conductance time constant), γ_J is a coefficient to control the strength of the conductance leak, and $\phi(\cdot)$ is a nonlinear transform applied to the error message input pool (in this work, we use the identity $\phi(v) = v$). Notice that, unlike in standard spiking neural networks, which are typically designed to be feedforward in nature, the SpNCN operates like a recurrent network, except that, instead of previous activity states, error messages are now propagated across the recurrent synapses. Furthermore, the state of the current variable $\mathbf{J}^\ell(t)$ is interpolated smoothly using the factor κ , inspired by the neuronal model of [71].

The general key components of the framework specified above are illustrated in Figure 1. All that remains is to define the third computation of an NCN, which, interestingly enough, can still be done without having yet specified a concrete SRM for the SpNCN.

Spike-Triggered Local Representation Alignment: In the presence of time-varying input, we propose adapting the synaptic connections of the SpNCN using a new form of the coordinated local learning rule, local representation alignment (LRA) [74, 77, 75], that has been successfully applied to modern-day, second generation artificial neural systems. This learning rule, which we will call *Spike-Triggered LRA* (ST-LRA), is an event-driven update which means that the presence of a binary spike will trigger an adjustment of the synapses for the relevant predictor neurons. Given that the predictions within the neural system are made in parallel to one another, once a hypothesis for any particular layer is generated, the corresponding error neurons e_i^ℓ are able to immediately perform the needed mismatch comparison (between the current state of the target area and prediction). The nature of the model’s prediction mechanism also entails parallel computation of weight updates – once the mismatch signal has been computed (Equation 2), a weight update for a layer ℓ of neurons may be readily computed.

⁴Note that in [29], the message passing done by superficial pyramidal cells is referred to as “backwards” transmission while the deep pyramidal cell message passing is referred to as “forwards” transmission. However, in the SpNCN/NCN, these directions are “flipped” – our error weights do the work of “backwards” transmission and the prediction weights do the work of “forwards” transmission. Nonetheless, for the SpNCN framework, it is more intuitive to instead think of message passing as moving vertically where prediction weights generate top-down expectations and error weights relate corrective signals, more like [88].

Much like a Hebbian update rule [39], ST-LRA makes use of readily available local information, making it biologically-plausible and much more hardware-friendly. The predictive weights for any layer W^ℓ , as well as its corresponding set of error weights E^ℓ , are updated as follows:

$$\Delta W^\ell = \mathbf{e}^{\ell-1}(t) \cdot (\mathbf{s}^\ell(t))^T, \quad \Delta E^\ell = -\beta (\mathbf{s}^\ell(t) \cdot (\mathbf{e}^{\ell-1}(t))^T) \quad (5)$$

where β is a coefficient that controls how quickly the error weights evolve, and usually can be set to a value close to one, such as $\beta = 0.9$. Notably, simulation speed of the SpNCN could be improved by reusing the already computed forward weight updates, i.e., $\Delta E^\ell = -\beta (\Delta W^\ell)^T$ (the error weight update is simulated using the weighted transpose of the forward weight update). where only outer products are needed to compute the relevant weight displacement matrix ΔW^ℓ . Interestingly enough, this LRA update, which could be viewed as an error-driven Hebbian rule [41, 75], works similarly to the classical delta rule [98] and the prescribed error rule [57, 5]. Using an LRA update in a neural model simply means that one is committed to accepting that there are neurons that are tasked solely with mismatch computations. Fortunately, in the brain, evidence of the existence of these error neurons has been found, especially in visual cortical circuits [63, 14, 6, 103, 26]. Furthermore, much in line with the hard/soft weight bounding employed in existing spike-timing rule simulations, we control for potential weight value explosion by bounding the Euclidean-norm of the vector columns of each weight matrix to a maximum length of 20. Biologically, this type of normalization could exist as a result of limited resource-availability for the actual process of synaptic adjustment. Once updates are computed, weight matrices would be updated via a single weighted step (similar to stochastic gradient descent): $W^\ell \leftarrow W^\ell - \alpha_u \Delta E^\ell$ and $E^\ell \leftarrow E^\ell - \alpha_u \Delta W^\ell$. α_u is the step size used in taking a step in the direction of the weight displacement (or ‘‘proxy gradient’’).

The synaptic evolution of the SpTNCN, under ST-LRA, is markedly different from spike-timing dependent plasticity (STDP) [58, 8, 9], which is more commonly used to adjust synaptic weight values in SNNs. However, while the SpNCN uses a discrepancy reduction-based approach to adaptation, there is no reason why it could not also be combined with the online form of STDP. Given that the brain is likely to employ different kinds of adjustment rules, doing so might allow for the fusion of both generative and discriminative knowledge when rapidly processing time-varying data points, which aligns with previous work that has empirically shown the benefits of doing so in statistical learning setups [70, 71, 81, 79, 78, 72, 73]. One can combine ST-LRA with online STDP through a convex combination, similar in spirit to [72]. Formally, the rule would be defined as:

$$\Delta W^\ell = (1 - \lambda) (\mathbf{e}^{\ell-1}(t) \cdot (\mathbf{s}^\ell(t))^T) - \lambda (A_+(W^\ell) (\mathbf{s}^{\ell-1}(t) \cdot (\mathbf{z}^\ell(t))^T) + A_-(W^\ell) (\mathbf{z}^{\ell-1}(t) \cdot (\mathbf{s}^\ell(t))^T)) \quad (6)$$

where λ is a coefficient introduced to control the strength of the STDP term throughout synaptic weight evolution. $A_+(W^\ell)$ and $A_-(W^\ell)$ are elementwise functions meant to introduce the soft (or hard) weight bounds generally used when training pure STDP-based SNNs.

With hypothesis generation, error-correction, and weight adaptation fully specified, all that remains is to decide on an SRM $f_{srn}(\cdot)$ to fully define a concrete SpNCN model. In the appendix, we present a full algorithmic specification for a general SpNCN that uses any kind of SRM neuronal model. We will next describe the SRM that we will focus on in this paper. However, once again, we note that better, more complicated choices of the SRM might facilitate different behavior and more closely mimic other important properties of biological neural circuitry.

The Leaky Integrate-and-Fire SRM: The SRM $f_{srn}(\mathbf{v}^\ell(t), \mathbf{J}^\ell(t))$ we chose to implement is the leaky integrate-and-fire (LIF) [24], which entails modeling neurons as leaky integrators of their current inputs. This integration over time, for a block ℓ of neurons, is specified by the following differential equation:

$$\tau_m \frac{\partial \mathbf{v}^\ell}{\partial t} = -\gamma_m \mathbf{v}^\ell(t) + R_m \mathbf{J}^\ell(t) \quad (7)$$

where R_m is the corresponding membrane resistance (for any single cell in the entire system), τ_m is the membrane time constant (specifically set as $\tau_m = R_m C_m$, where C_m is the membrane capacitance), γ_m is a coefficient that controls the strength of the leak. The above equation, in actuality, describes a simple resistor-capacitor (RC) circuit, with the leakage resulting from the resistor. The current $\mathbf{J}^\ell(t)$ is integrated over time by the capacitor, which is placed in parallel to the resistor. In order to simulate leaky integrator neuron dynamics with Equation 7, we approximate the differential equation with the forward Euler method to compute the value of the voltage $\mathbf{v}^\ell(t)$. This calculation proceeds as follows:

$$\mathbf{v}^\ell(t + \Delta t) = \mathbf{v}^\ell(t) + \frac{\Delta t}{\tau_m} (-\gamma_m \mathbf{v}^\ell(t) + R_m \mathbf{J}^\ell(t)) \quad (8)$$

where Δt is the integration time constant (replacing the ∂t in the original differential equation).

In order to generate a spike, a threshold \mathbf{v}_{thr} must be chosen against which $\mathbf{v}^\ell(t)$ is compared. As the voltage $\mathbf{v}^\ell(t)$ accumulates over time, a neuron will emit a spike once its voltage exceeds \mathbf{v}_{thr} (in the simulations of this paper, we

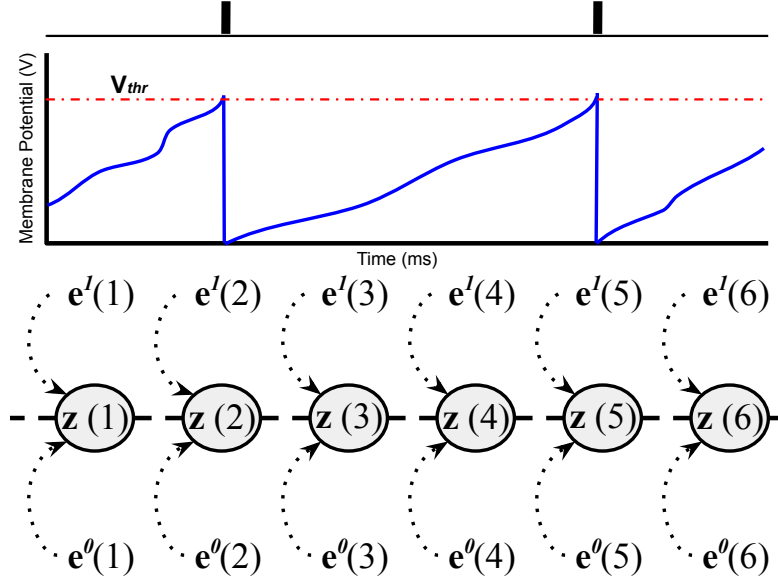


Figure 2: A demonstration of a spike train generated by a single LIF neuron within the SpNCN over time. Bottom diagram shows the actual neuron receiving error signals at simulated time steps, the middle diagram shows the membrane potential (voltage) at each simulated step, and the topmost diagram displays the actual (binary) spike if the membrane potential exceeds the threshold v_{thr} .

operate in the $[0, 1]$ decivolt range). Upon emitting a spike (yielding a value of 1), a neuron’s voltage variable is reset to 0, our chosen voltage resting rate for this paper’s experiments. A spike vector is simply created via the following vector elementwise comparison: $\mathbf{s}^\ell(t) = \mathbf{v}^\ell(t) \geq v_{thr}$. In Figure 2, an LIF unit’s spike generation process is depicted (with the leak turned off, $\gamma = 0$, and no refractory period).

Furthermore, we incorporate an absolute refractory period into our implementation of the LIF SRM. In short, after an LIF neuron spikes, a period of t_r simulation time must pass before a build-up of potential is allowed again and the value of the neuron is fixed to 0 until the refractory period has ended. In this work, we fix the absolute refractory period to be $t_r = 1$ ms (unless noted otherwise).

Input Representation: To present data to the SpNCN, the input patterns that are clamped to its sensors are transformed on-the-fly to adhere to a Poisson spike-train. In the case of images, which could be randomly shuffled static pictures or ordered frames of a video, two-dimensional (2D) pixel grids are flattened to 1D vectors. The values of each pattern vector \mathbf{x} are then normalized to lie in the range $[0, 1]$ by dividing the scalar values along each dimension by the maximum pixel value 255 (since pixels naturally live in the range $[0, 255]$). To obtain Poisson spike rates, the normalized pattern vectors are then scaled by a maximum spiking rate K , yielding a rate vector \mathbf{r} , where K is in Hertz (Hz), meaning that each dimension of the pattern vector corresponds to a sensory neuron that spikes K times per second.

Using the converted input Poisson spike rates obtained from the step above, we then generate at any time t a binary spike vector representation \mathbf{s}_t^0 of the data point \mathbf{x} via the following: $\epsilon_t < (\frac{\Delta t}{1000} \mathbf{r})$ (the factor $\frac{1}{1000}$ enforces the millisecond, or ms, as our fundamental unit of time). As a result, if one specifies that a particular pattern vector \mathbf{x} is to be presented to the SpNCN for a total stimulus time of 1 second, or 1000 ms, then for a time integration constant of $\Delta t = 1$ ms, we would obtain a spike train of 1000 binary vectors that temporally encode the pattern. Note that, just as it is done for the internal layers of the SpNCN, a trace filter is applied to the binary spike train stimulus.

3 Experiments

In this section, we present a set of experiments that test the SpNCN’s ability to generate and classify patterns, in both supervised and semi-supervised scenarios, and, furthermore, its ability to retain knowledge over a task sequence.

3.1 Continual Signal Chasing: The Bouncing Ball Problem Revisited

When processing sensory input vectors from a stream, the SpNCN is engaged in the process of “signal chasing”, constantly predicting the sensory input it is about to receive and then error-correcting its internal state before receiving the next input. In most applications where sensory streams are prevelant, e.g., autonomous vehicles and robotics, this

means the SpNCN will make relevant predictions based on a continual, shifting representation of its environment which is further encoded in binary spike train patterns.

To evaluate how well the SpNCN chases signals in a data continuum, we adapt the classic bouncing ball problem often used to evaluate generative models in statistical learning research, such as temporal variants of Boltzmann machines [94, 92] and neural predictive coding models [74]. The problem entails predicting frames of pre-generated video snippets of the simulated rudimentary physics of three balls bouncing around in a box. Specifically, we implement it as continuously running stochastic process to generate streams of user-specified length, the output of which might serve as a new simple benchmark for evaluating the online adaptivity of spiking neural models. We set up our generator to create a single long-running video of $n = 3$ balls bouncing around in a pixel grid forcing the neural system to learn how to predict/generate incoming frames given its current state. Each gray-scale video frame is 16×16 pixels and each frame is converted to a 64 Hz Poisson spike train. For this experiment, we generated a small finite stream of $K = 2000$ frames. A 2-layer SpNCN is adapted online using ST-LRA on the stream for the first 1000 frames. For the last 1000 frames, we deactivate the learning rule in order to test if the SpNCN is still able to generate patterns without synaptic weight adjustment. The simulation time step used for this experiment was $\Delta t = 0.1$ ms (simulation consisted of 600000 discrete steps) and stimulus (video frame) presentation time was $T_{st} = 30$ ms. The SpNCN consists of 400 LIF units in the first layer and 100 units in the second layer. We use a leak scale of $\gamma = 0.25$ (and no refractory period for this simulation).

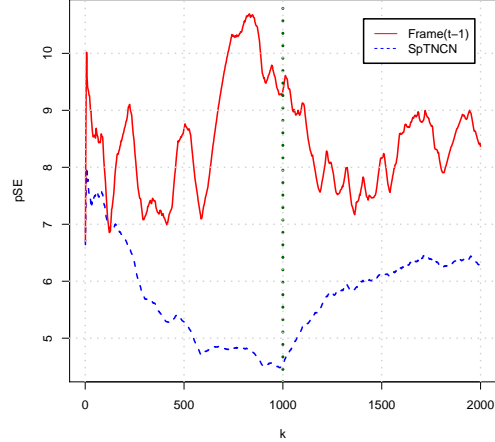


Figure 3: SpNCN tracking performance on the bouncing ball stream problem (pSE over video frame k). The vertical (green) dotted line marks the point when synaptic change was inhibited.

In online learning [31] it is common practice to record an evolving model’s prediction error on a single sample presented at a particular instant in time and update a running, often decaying average of cumulative error. This is often referred to as prequential error [31, 79]. Our variant of this metric, prequential squared error (pSE), is calculated as follows:

$$P_{\alpha}(i) = \frac{\sum_{k=1}^i \alpha^{i-k} \left((\hat{\mathbf{x}} - \mathbf{x})^T \cdot (\hat{\mathbf{x}} - \mathbf{x}) \right)}{\sum_{k=1}^i \alpha^{i-k}} \quad (9)$$

where $0 \ll \alpha \leq 1$ (we set $\alpha = 0.995$ for this experiment). $\hat{\mathbf{x}}$ is the expected value of the SpNCN’s prediction, $\mathbb{E}[\mathbf{z}_{\mu}^0]$, of the k -th target video frame, estimated as the empirical average $\sum_{t=1}^{T_{st}} \mathbf{z}_{\mu}^0(t)$ over the stimulus presentation period.

In Figure 3, we plot the SpNCN’s learning curve (pSE) across the entire simulated 30 second period. To check that the SpNCN is indeed learning how predict its input over time, we also plot the pSE of the *Frame(t-1)* model as a reference, which simply predicts the next frame by copying the exact previously seen frame (and often makes for a strong baseline model). As observed in the figure, the SpNCN is able to maintain a reasonably good reconstruction of the target signal while consistently doing better than the baseline. The SpNCN reached an average $pSE = 6.672$ whereas the baseline predictor reaches a $pSE = 10.225$. More importantly, we should emphasize that over the 300000 discrete simulation steps taken (for the 1000 training frames, each presented 30 ms), only 46,393 synaptic weight updates were made for $\{W1, E1\}$ and only 28,998 updates were made for $\{W2, E2\}$. This means that the number of weight adjustments is quite sparse over time which might prove to be a significant economy in the employment of real-time hardware systems. Furthermore, the fact that upper layer (second LIF layer) updates its synapses fewer times than the lower layer (first LIF layer) could be likened to the process of slow feature analysis [99], since higher-level feature detectors would be (roughly) operating on a slower-moving time-scale than the lower-level units.

3.2 Image Categorization Tasks:

We next investigate a more complex, high-dimensional classification challenge using the MNIST database⁵. This dataset contains images of 28×28 gray-scale pixel grids (feature values in the range of $[0, 255]$). Fashion MNIST [100], on the other hand, contains 28×28 grey-scale images of 10 classes of clothing items instead of digits or characters. Data setup was the same as was described for MNIST in the previous section. We also investigated the Stanford Optical Character

⁵<http://yann.lecun.com/exdb/mnist/>.

Table 1: Generalization error of various spiking networks on MNIST. The performance of our SpNCN and implemented SNN baselines (labeled with “impl.”) were measured over 10 trials. Models below the double line are online models.

Model	Preprocess?	Type	Performance
Dendritic Neurons [43]	Yes	Rate-based	9.7%
Spiking RBM [61]	No	Rate-based	11.0%
Spiking RBM [67]	Yes	Rate-based	5.9%
Spiking CNN, BP [20]	No	Rate-based	0.9%
Spiking RBM [65]	Yes	Rate-based	7.4%
Spiking RBM [65]	Yes	Spike-Based	8.1%
Spiking CNN [102]	Yes	Spike-Based	8.7%
2-Layer SNN [13]	Yes	Spike-Based	3.5%
ML H-SNN [7]	Yes	Spike-Based	8.4%
2-Layer SNN [85]	No	Spike-Based	6.5%
2-Layer SNN [19]	No	Spike-Based	5.0%
syn-SNN (STDP) [36]	No	Rate-based	3.27%
SNN-LM [37]	No	Spike-Based	5.93%
2-Layer SNN, 3 passes [19]	No	Spike-Based	~ 17.1%
Online SNN-LM [37]	No	Spike-Based	6.61%
Online SCNN [95]	No	Spike-Based	4.76%
SNN, df-DRTP [28] (impl.)	No	Spike-Based	40.13 ± 0.35%
SNN, df-BFA [91] (impl.)	No	Spike-Based	9.38 ± 0.12%
SpNCN (ours)	No	Spike-Based	4.72 ± 0.11%

Table 2: Generalization error of various online spiking networks on Fashion MNIST, Stanford OCR, and Caltech 101 datasets.

Model	Preprocess?	Type	Fashion MNIST Performance	Stanford OCR Performance	Caltech 101 Performance
ANN, BP	No	Rate-based	12.98% [75]	37.01 ± 1.19%	44.77 ± 1.22%
syn-SNN (STDP)	No	Rate-based	15.35% [36]	–	–
SNN, df-DRTP [28] (impl.)	No	Spike-Based	45.27 ± 0.26%	92.19 ± 0.03%	77.75 ± 0.14%
SNN, df-BFA [91] (impl.)	No	Spike-Based	25.65 ± 0.12%	94.15 ± 0.51%	63.64 ± 0.41%
SpNCN (ours)	No	Spike-Based	15.71 ± 0.05%	49.58 ± 0.15%	57.85 ± 0.40%

Recognition (OCR)⁶ and Caltech 101 Silhouettes⁷ datasets, both of which were in binary vector form and thus required no normalization. For all datasets, the image vectors were converted to Poisson spike trains by first multiplying the (normalized) vector by a maximum desired spike rate, i.e., 63.75 (to be in accordance with [19]). Spikes were then generated by sampling on-the-fly. Images were presented for stimulus time of $T_{st} = 100$ ms.

SpNCN models trained consisted of 4 layers of LIF units (each with 1000 units). The absolute refractory period was 1 ms and the integration time constant was $\Delta t = 0.25$ ms. Step size $\alpha = 0.0025$ and $\beta = 1.0$. We furthermore implemented a standard SNN trained online by broadcast feedback alignment (BFA), specifically a derivative-free variant [91] (*df-BFA*) to ensure that the SNN can employ the exact same LIF SRM that the SpNCN uses. This baseline is referred to as *SNN, df-BFA* in all tables. Furthermore, we implemented a derivative-free variant of another broadcast alignment-like algorithm known as direct random target projection (*df-DRTP*) [28] as an additional alternative to training SNNs. In the appendix, we describe the details of our *df-BFA* and *df-DRTP* implementations.

In Table 1, we report the generalization performance (on each dataset’s respective test set), averaged over 10 trials. Note that in our evaluation, the SpNCN’s reported generalization is the result of letting it adapt to the MNIST training set a single time, since our goal is to evaluate the model’s streaming performance exclusively. The spiking models we compare its performance are ones that were trained over multiple passes (epochs) over the database. For an approximation of how a performant SNN trained by STDP performs in a similar setting, we add a line to the table with the value explained in [19] (the original paper reported only 3 passes over MNIST, which means it has an advantage over the SpNCN of seeing the MNIST data at least two more times). The performance of an STDP-driven SNN is significantly lower than the SNN trained for 15 epochs on MNIST (the last model performance just above the double line in Table 1), which was a wide model containing 6400 neurons, thus much wider than the streaming SpNCNs we experimented with in this study. We furthermore compare to a powerful spiking convolutional network (SCNN) [95].

⁶<http://ai.stanford.edu/~btaskar/oct/>⁷<https://people.cs.umass.edu/~marlin/data.shtml>

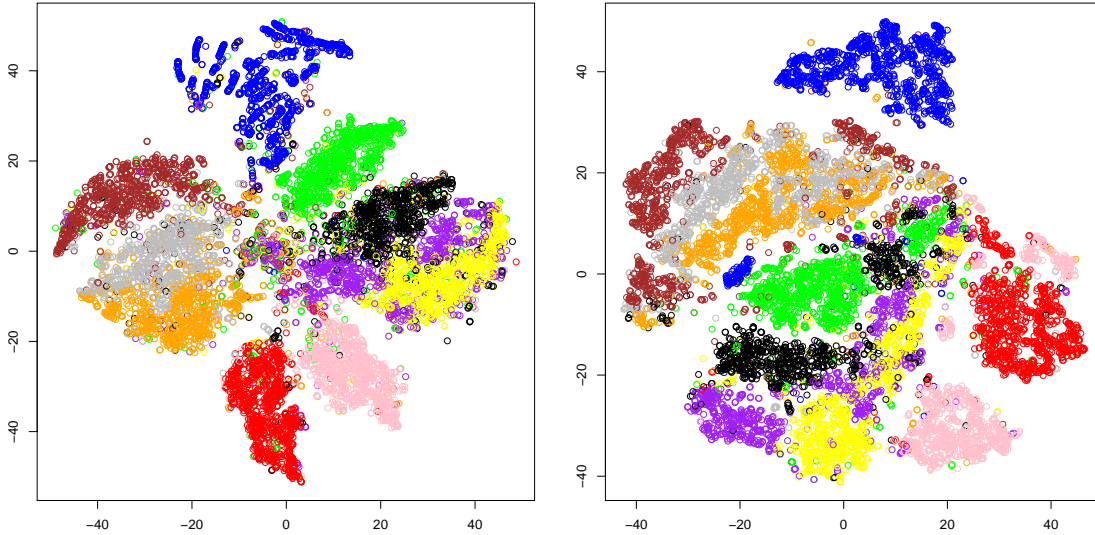


Figure 4: t-SNE visualizations of a fully supervised SpNCN (left) and an unsupervised SpNCN (right) (for MNIST).

Observe that in the case of MNIST, our proposed SpNCN actually performs comparably to one of the most powerful SNN models. This is interesting for two reasons: 1) the SpNCN is not trained at all with any form of STDP and 2) the SpNCN is trained online, unlike most of the models we compare to (which are trained by passing over the MNIST dataset multiple times). We should note that state-of-the-art performance for SNNs on MNIST include 2.8% [64] and 1.6% [49]. However, both of these models (and many like them) are convolutional in nature and make use of complex learning mechanisms including reinforcement learning. In terms of fully-connected SNN architectures, the SpNCN is quite competitive (even as an online learning algorithm) and, notably, is comparable to the performance of the more complex SCNN [95]. Note that it would be fruitful to incorporate additional learning rules from recent work [49, 64] to further improve the SpNCN’s generalization ability. As mentioned before, there is no reason why the SpNCN’s ST-LRA update rule could not be combined with other learning rules, such as the more common STDP.

Finally, in Table 2 we report training a 4-layer SpNCN on Fashion MNIST, Stanford OCR, and Caltech 101. While current research has not focused on evaluating SNNs on Fashion MNIST (and has not examined Stanford OCR and Caltech 101), we provide, for reference, a classical backprop-trained non-spiking ANN. We note that while the SpNCN does not exactly match the non-spiking model’s performance (on any of these datasets), it does come close (and is comparable to syn-SNN) which is impressive for a more difficult benchmark like Fashion MNIST. Furthermore, the SpNCN consistently outperforms the other SNNs trained with *df-BFA* and *df-DRTP* on Stanford OCR and Caltech 101.

In order to examine the quality of the spike-train representations acquired by a trained SpNCN, we visualize its approximate layerwise embeddings when it is presented with (MNIST) test images. Specifically, we extract a vector embedding for an image by computing the rate-code equivalent of the corresponding spike-train, for any particular layer ℓ , via the following:

$$\mathbf{c}^\ell = \frac{\gamma_c}{N_c} \sum_{t=1}^{T_{st}} \mathbf{s}^\ell(t), \text{ where, } 0 < \gamma_c \leq 1 \quad (10)$$

where γ_c is a coefficient used to control how well the approximate encoding fits into the range of $[0, 1]$ (we set $\gamma_c = 1$ for this study) and N_c is the number of cycles over T_{st} , or total number of steps taken within the stimulus time. The resulting rate-code equivalent embeddings are plotted in Figure 4 using t-SNE to perform the mapping from the layer’s dimension to 2D (t-SNE was ran with a perplexity target of 30 for 100 iterations after an initial PCA projection). We present a t-SNE visualization of an SpNCN that was trained with all of the training labels (left) and an SpNCN that was trained with none of the training labels (right) to compare representations it acquires in either purely supervised or unsupervised settings (since the SpNCN can learn without labels since it aims to predict the input image as well). Interestingly enough, we see that both supervised and unsupervised SpNCN variants acquire representations that cluster together quite nicely. However, unsurprisingly, the supervised SpNCN individual digit representations that are much better separated, largely owing to the fact it has access to the extra supervised learning signal.

Online Semi-Supervised Learning: One of the many interesting properties of the SpNCN (and, in truth, any type of NPC-based model [73]) is that it is more general model than most SNNs (or ANNs) which are designed to learn

Table 3: Semi-supervised error (10-trial means) of a 2-layer SpNCN on MNIST and Fashion MNIST (FMNIST), varying the proportion of samples that arrive labeled in the stream (first column is fully supervised for reference).

MNIST Model	0%	90%	95%	99%	99.5%
SNN, df-BFA	11.16 \pm 0.07%	16.07 \pm 0.11%	17.04 \pm 0.16%	29.00 \pm 0.11%	37.35 \pm 0.11%
SpNCN	7.15 \pm 0.19%	13.64 \pm 0.15%	17.48 \pm 0.21%	23.44 \pm 0.16%	24.082 \pm 0.23%
FMNIST Model	0%	90%	95%	99%	99.5%
SNN, df-BFA	24.80 \pm 0.07%	38.82 \pm 0.07%	34.84 \pm 0.08%	39.77 \pm 0.06%	50.02 \pm 0.07%
SpNCN	18.67 \pm 0.13%	21.44 \pm 0.15%	21.01 \pm 0.13%	24.39 \pm 0.15%	29.37 \pm 0.18%

a specialized, discriminative mapping from x to y . This means that in a more realistic setting where patterns in the stream do not always have labels, the SpNCN should still be able to extract information from whatever portion of sensory input is available and adapt its synapses accordingly.

To simulate this setting, we train several smaller SpNCNs (two layers, first layer with 400 LIF units, second layer with 200 LIF units) on variants of the MNIST database with different proportions of samples selected to be “unlabeled”, i.e., the label vectors for each of these samples are never used in the simulation. In Table 3, we present the results of this simulation and observe that the SpNCN maintains a rather reasonably low error even as the number of labeled samples dwindles. We compare the SpNCN to a 2-layer standard SNN trained via *df-BFA* with the same number of total weights as the two-layer SpNCN. The SNN’s performance degrades more severely than the SpNCN as the proportion of unlabeled samples in the stream increases. This makes sense since the SNN is focused with only learning a discriminative function and, as a result, cannot make use of unlabeled samples. An SpNCN, on the other hand, works more like a hybrid discriminative-generative model [23, 53, 81, 79, 78], where older work demonstrated that in ANNs, learning a generative model jointly with a discriminative mapping can facilitate stronger generalization even when the number of labels is small. In essence, the SpNCN extends the idea of hybrid learning to spike train encodings, opening up interesting directions for future work to take when considering semi-supervised learning.

On Catastrophic Forgetting: When trained on more than one dataset, or “task”, sequentially, ANNs are known to succumb to catastrophic interference or catastrophic forgetting, where recently-seen information blindly overwrites prior knowledge already encoded in a neural system’s synapses [59, 89, 55]. A great deal of work exists in attempting to combat this difficult problem, however, the ANN investigations have primarily been continuously graded and involve all internal neuronal processing elements in the processing of each and every pattern, i.e., the ANN uses heavily dense activity patterns. The resulting “cross-talk” between an ANN’s neurons is often depicted to be one source of catastrophic interference and, classically [27], as well as recently [73], sparsity has been argued to be one biologically-inspired solution to improve ANN memory retention. Since spiking neural architectures naturally make use of very sparse codes, we are interested in determining if this natural sparsity alone might help in mitigating the amount of forgetting a neural system experiences when adapting online to a sequence of different tasks.

To experimentally evaluate our proposed SpNCN’s ability to aggregate knowledge across multiple, distinct tasks, we adapt the Split MNIST and NotMNIST continual learning benchmarks to the spike-train continuous time setting. Split MNIST is effectively just the MNIST (described earlier) but with the sample images split into five subsets of consecutive digit pairs, where a task corresponds learning to distinguish between two different objects. The subsets are arranged in a particular order, i.e., a task sequence stream, presenting a particularly difficult learning challenge to the learner since there is cross-talk between digit classes in the output layer due to changes in the label distribution over subsets of digit samples. Split NotMNIST is identical to Split MNIST except that, instead of digits, the subsets of data pertain to characters of varying fonts/glyphs (letters A-J).⁸ We do not make use of task descriptors, which means that the system is given no explicit knowledge of task order and task boundaries. Furthermore, we introduce “task boundary fuzzing” – instead of presenting samples from each task strictly in a certain order, during the processing of samples from one task’s stream, we randomly inject a small proportion of samples from other tasks. We evaluate performance based on average accuracy (ACC), which essentially measures a model’s overall generalization across a sequence of tasks after reaching the end of the data continuum stream. We report our ACC measurements in Table 4 on both benchmarks for an SNN trained

Table 4: Generalization metrics (10 trials) for lifelong learning benchmarks: Split MNIST and NotMNIST. We measure average accuracy (ACC), where a higher value is better.

	MNIST ACC	NotMNIST ACC
ANN, BP	58.35%	67.69%
SNN df-BDA	62.490 \pm 0.001%	69.688 \pm 0.002%
SpNCN	76.455 \pm 0.002%	77.945 \pm 0.003%

⁸<http://yaroslavvb.blogspot.com/2011/09/notmnist-dataset.html>

with *df-BFA* and our proposed SpNCN (both architectures have 3 hidden layers of 1000 LIF neurons). We add as a reference the performance of a continuously-graded ANN with the same number of parameters trained via backprop. We emphasize that our goal is not necessarily to reach modern-day state-of-the-art ANN ACC levels on this benchmarks, but rather, to experimentally determine if a spiking system’s sparse representations might help in reducing forgetting.

As observed in our results, we see that neural processing based on spike trains does indeed appear to reduce forgetting to a degree, though not strongly. The SNN (trained with *df-BFA*) does exhibit an improvement in ACC over a standard real-valued ANN while the SpNCN exhibits the best ACC overall. However, while memory retention appears to be improved by simply switching to the use of a raw spiking neural architecture over a real-valued ANN, it is important to note that we do not claim that the natural sparsity of a spiking neural system, including our own proposed SpNCN, is enough to solve the grand challenge of catastrophic forgetting (as evidenced by the fact that ACC is not at the level of recently specialized, heavily engineered ANNs trained on the same benchmarks). Rather, it is likely that this sparsity will mix favorably with recent engineering efforts in improving memory retention in real-valued ANN systems, especially when used in tandem with architectures are modular, allowing the design of specialized forms of memory that will dramatically reduce further neural cross-talk.

4 Discussion and Limitations

While the proposed SpNCN represents an important step towards the bridging of practical machine learning and computational neuroscience, there are many aspects of our model, in its current form, that differ too greatly from known neurobiology. While these elements can be addressed, incorporating them might introduce further challenges in developing a model that generalizes well while still adhering to constraints that the properties of real biological neurons satisfy. One such element is the fact that excitatory and inhibitory synaptic weights in our SpNCN are not distinctly separated and are essentially “globbed” together. In the brain, it is a common pattern for there to only be a certain proportion of neurons that are inhibitory (about 20%) while the rest are excitatory. Furthermore, while learning using ST-LRA, the signs of the SpNCN’s weights could very possibly change during the course of model evolution. To remedy this, the SpNCN’s input current variable block \mathbf{J} could instead be formulated to separate out the excitatory and inhibitory input channels. In addition, a constraint could be imposed that fixes the signs of simulated synapses at model initialization with a biologically realistic proportion of weights assigned negative signs. Further inspiration from neurocognitive architectures such as LEABRA [71] or spiking neural simulators such as BRIAN [33] could help in cleanly integrating these design elements into our framework.

While the LIF SRM we specifically experimented with is quite useful, especially with the inclusion of the absolute refractory period, there are still additional mechanisms that should be modeled in order to build a proper neuronal simulation. Beyond the inclusion of a relative refractory period, modeling other important neuronal dynamics such as accommodation (a neuron fatigues, or becomes less and less active for the same excitatory input) and hysteresis (a neuron remains active for a period of time even if the excitatory input fades or is removed) would prove interesting and could be easily done by modifying the LIF differential equation we specified earlier [71]. Alternatively, one could simply swap out the LIF SRM used within the SpNCN with a more realistic (though computationally more expensive) neuronal model, such as those used in [46, 42].

5 Conclusions

In this paper, we proposed the spiking neural coding network, a model that is composed of leaky integrate-and-fire neurons, and its learning algorithm for adjusting synaptic weight strengths incrementally. The model was formulated under a general framework that can naturally accommodate simulated neuronal models of varying complexity, ranging from the leaky integrate-and-fire unit used in this article to those based on the Hodgkin-Huxley coupled differential equations. Simple pattern classification and signal tracking experiments demonstrate the potential generalization ability of our model in the realm of online, continuous-time based learning.

The spiking neural coding network works by continuously chasing targets, constantly making guesses as to activities of its internal neuronal units and then correcting its states to ensure better predictions are made in the future. Even though it is trained purely online, the model is competitive with many powerful SNNs learned with STDP or other approaches. Furthermore, our model exhibits better computational economy and is more biologically-plausible than modern-day (non-spiking) artificial neural networks. Future work will entail investigating the further development of the proposed spiking network for use in more complex applications, especially those involving motor control, which would be of immense value to robotics research. In addition, the direct integration and evaluation of the proposed spiking system on neuromorphic hardware, where the energy efficiency gains will be most prominent and critical, will be explored.

Acknowledgements

We would like to thank Chris Eliasmith, Terrence Stewart, and Peter Blouw for useful discussions on the internal mechanics of NENGO and the dynamics of spiking neurons, which have helped shaped many of the ideas behind the custom Scala code/implementation that drives this paper. We also thank Alexander Ororbia (Sr) for valuable comments/suggestions for the early drafts of this paper.

References

- [1] ADESNIK, H., AND SCANZIANI, M. Lateral competition for cortical space by layer-specific horizontal circuits. *Nature* 464, 7292 (2010), 1155.
- [2] ANGELA, J. Y., AND DAYAN, P. Uncertainty, neuromodulation, and attention. *Neuron* 46, 4 (2005), 681–692.
- [3] ATAL, B., AND SCHROEDER, M. Predictive coding of speech signals and subjective error criteria. *IEEE Transactions on Acoustics, Speech, and Signal Processing* 27, 3 (1979), 247–254.
- [4] BASTOS, A. M., USREY, W. M., ADAMS, R. A., MANGUN, G. R., FRIES, P., AND FRISTON, K. J. Canonical microcircuits for predictive coding. *Neuron* 76, 4 (2012), 695–711.
- [5] BEKOLAY, T., KOLBECK, C., AND ELIASMITH, C. Simultaneous unsupervised and supervised learning of cognitive functions in biologically plausible spiking neural networks. In *Proceedings of the Annual Meeting of the Cognitive Science Society* (2013), vol. 35.
- [6] BELL, A. H., SUMMERFIELD, C., MORIN, E. L., MALECEK, N. J., AND UNGERLEIDER, L. G. Encoding of stimulus probability in macaque inferior temporal cortex. *Current Biology* 26, 17 (2016), 2280–2290.
- [7] BEYELER, M., DUTT, N. D., AND KRICHMAR, J. L. Categorization and decision-making in a neurobiologically plausible spiking network using a stdp-like learning rule. *Neural Networks* 48 (2013), 109–124.
- [8] BI, G.-Q., AND POO, M.-M. Synaptic modifications in cultured hippocampal neurons: dependence on spike timing, synaptic strength, and postsynaptic cell type. *Journal of neuroscience* 18, 24 (1998), 10464–10472.
- [9] BI, G.-Q., AND POO, M.-M. Synaptic modification by correlated activity: Hebb’s postulate revisited. *Annual review of neuroscience* 24, 1 (2001), 139–166.
- [10] BOAHEN, K. Neuromorphic microchips. *Scientific American* 292, 5 (2005), 56–63.
- [11] BOERLIN, M., MACHENS, C. K., AND DENÈVE, S. Predictive coding of dynamical variables in balanced spiking networks. *PLoS computational biology* 9, 11 (2013), e1003258.
- [12] BOHTE, S. M., KOK, J. N., AND LA POUTRE, H. Error-backpropagation in temporally encoded networks of spiking neurons. *Neurocomputing* 48, 1-4 (2002), 17–37.
- [13] BRADER, J. M., SENN, W., AND FUSI, S. Learning real-world stimuli in a neural network with spike-driven synaptic dynamics. *Neural computation* 19, 11 (2007), 2881–2912.
- [14] BROWN, M. W., AND AGGLETON, J. P. Recognition memory: what are the roles of the perirhinal cortex and hippocampus? *Nature Reviews Neuroscience* 2, 1 (2001), 51.
- [15] CHRISTOPHE, F., MIKKONEN, T., ANDALIBI, V., KOSKIMIES, K., AND LAUKKARINEN, T. Pattern recognition with spiking neural networks: a simple training method. In *SPLST* (2015), pp. 296–308.
- [16] DAVIES, M., SRINIVASA, N., LIN, T.-H., CHINYA, G., CAO, Y., CHODAY, S. H., DIMOU, G., JOSHI, P., IMAM, N., JAIN, S., ET AL. Loihi: A neuromorphic manycore processor with on-chip learning. *IEEE Micro* 38, 1 (2018), 82–99.
- [17] DE LA ROCHA, J., DOIRON, B., SHEA-BROWN, E., JOSIĆ, K., AND REYES, A. Correlation between neural spike trains increases with firing rate. *Nature* 448, 7155 (2007), 802.
- [18] DEVLIN, J., CHANG, M.-W., LEE, K., AND TOUTANOVA, K. Bert: Pre-training of deep bidirectional transformers for language understanding. *arXiv preprint arXiv:1810.04805* (2018).
- [19] DIEHL, P. U., AND COOK, M. Unsupervised learning of digit recognition using spike-timing-dependent plasticity. *Frontiers in computational neuroscience* 9 (2015), 99.
- [20] DIEHL, P. U., NEIL, D., BINAS, J., COOK, M., LIU, S.-C., AND PFEIFFER, M. Fast-classifying, high-accuracy spiking deep networks through weight and threshold balancing. In *2015 International Joint Conference on Neural Networks (IJCNN)* (2015), IEEE, pp. 1–8.

- [21] DIEHL, P. U., ZARRELLA, G., CASSIDY, A., PEDRONI, B. U., AND NEFTCI, E. Conversion of artificial recurrent neural networks to spiking neural networks for low-power neuromorphic hardware. In *2016 IEEE International Conference on Rebooting Computing (ICRC)* (2016), IEEE, pp. 1–8.
- [22] DOYA, K. Metalearning and neuromodulation. *Neural Networks* 15, 4-6 (2002), 495–506.
- [23] DRUCK, G., PAL, C., MCCALLUM, A., AND ZHU, X. Semi-supervised classification with hybrid generative/discriminative methods. In *Proceedings of the 13th ACM SIGKDD international conference on Knowledge discovery and data mining* (2007), ACM, pp. 280–289.
- [24] ELIASMITH, C., AND ANDERSON, C. H. *Neural engineering: Computation, representation, and dynamics in neurobiological systems*. MIT press, 2004.
- [25] ELIASMITH, C., STEWART, T. C., CHOO, X., BEKOLAY, T., DEWOLF, T., TANG, Y., AND RASMUSSEN, D. A large-scale model of the functioning brain. *science* 338, 6111 (2012), 1202–1205.
- [26] FISER, A., MAHRINGER, D., OYIBO, H. K., PETERSEN, A. V., LEINWEBER, M., AND KELLER, G. B. Experience-dependent spatial expectations in mouse visual cortex. *Nature neuroscience* 19, 12 (2016), 1658.
- [27] FRENCH, R. M. Catastrophic forgetting in connectionist networks. *Trends in cognitive sciences* 3, 4 (1999), 128–135.
- [28] FRENKEL, C., LEFEBVRE, M., AND BOL, D. Learning without feedback: Direct random target projection as a feedback-alignment algorithm with layerwise feedforward training. *arXiv preprint arXiv:1909.01311* (2019).
- [29] FRISTON, K., AND KIEBEL, S. Predictive coding under the free-energy principle. *Philosophical Transactions of the Royal Society B: Biological Sciences* 364, 1521 (2009), 1211–1221.
- [30] FURBER, S. B., GALLUPPI, F., TEMPLE, S., AND PLANA, L. A. The spinnaker project. *Proceedings of the IEEE* 102, 5 (2014), 652–665.
- [31] GAMA, J., SEBASTIÃO, R., AND RODRIGUES, P. P. On evaluating stream learning algorithms. *Machine learning* 90, 3 (2013), 317–346.
- [32] GLOROT, X., AND BENGIO, Y. Understanding the difficulty of training deep feedforward neural networks. In *Proceedings of the thirteenth international conference on artificial intelligence and statistics* (2010), pp. 249–256.
- [33] GOODMAN, D. F., AND BRETTE, R. The brian simulator. *Frontiers in neuroscience* 3 (2009), 26.
- [34] GROSSBERG, S. Competitive learning: From interactive activation to adaptive resonance. *Cognitive science* 11, 1 (1987), 23–63.
- [35] HAGRAS, H., POUNDS-CORNISH, A., COLLEY, M., CALLAGHAN, V., AND CLARKE, G. Evolving spiking neural network controllers for autonomous robots. In *IEEE International Conference on Robotics and Automation, 2004. Proceedings. ICRA'04. 2004* (2004), vol. 5, IEEE, pp. 4620–4626.
- [36] HAO, Y., HUANG, X., DONG, M., AND XU, B. A biologically plausible supervised learning method for spiking neural networks using the symmetric stdp rule. *arXiv preprint arXiv:1812.06574* (2018).
- [37] HAZAN, H., SAUNDERS, D., SANGHAVI, D. T., SIEGELMANN, H., AND KOZMA, R. Unsupervised learning with self-organizing spiking neural networks. In *2018 International Joint Conference on Neural Networks (IJCNN)* (2018), IEEE, pp. 1–6.
- [38] HE, K., ZHANG, X., REN, S., AND SUN, J. Identity mappings in deep residual networks. In *European conference on computer vision* (2016), Springer, pp. 630–645.
- [39] HEBB, D. O., ET AL. The organization of behavior, 1949.
- [40] HINTON, G., DENG, L., YU, D., DAHL, G., MOHAMED, A.-R., JAITLEY, N., SENIOR, A., VANHOUCHE, V., NGUYEN, P., KINGSBURY, B., ET AL. Deep neural networks for acoustic modeling in speech recognition. *IEEE Signal processing magazine* 29 (2012).
- [41] HINTON, G. E., AND MCCLELLAND, J. L. Learning representations by recirculation. In *Neural information processing systems* (1988), pp. 358–366.
- [42] HODGKIN, A. L., AND HUXLEY, A. F. A quantitative description of membrane current and its application to conduction and excitation in nerve. *The Journal of physiology* 117, 4 (1952), 500–544.
- [43] HUSSAIN, S., LIU, S.-C., AND BASU, A. Improved margin multi-class classification using dendritic neurons with morphological learning. In *2014 IEEE International Symposium on Circuits and Systems (ISCAS)* (2014), IEEE, pp. 2640–2643.
- [44] HWU, T., ISBELL, J., OROS, N., AND KRICHMAR, J. A self-driving robot using deep convolutional neural networks on neuromorphic hardware. In *2017 International Joint Conference on Neural Networks (IJCNN)* (2017), IEEE, pp. 635–641.

- [45] INDIVERI, G., AND HORIUCHI, T. Frontiers in neuromorphic engineering. *Frontiers in Neuroscience* 5 (2011), 118.
- [46] IZHIKEVICH, E. M. Simple model of spiking neurons. *IEEE Transactions on neural networks* 14, 6 (2003), 1569–1572.
- [47] JADERBERG, M., CZARNECKI, W. M., OSINDERO, S., VINYALS, O., GRAVES, A., SILVER, D., AND KAVUKCUOGLU, K. Decoupled neural interfaces using synthetic gradients. In *Proceedings of the 34th International Conference on Machine Learning-Volume 70* (2017), JMLR. org, pp. 1627–1635.
- [48] JO, T., HOU, J., EICKHOLT, J., AND CHENG, J. Improving protein fold recognition by deep learning networks. *Scientific reports* 5 (2015), 17573.
- [49] KHERADPISHEH, S. R., GANJTABESH, M., THORPE, S. J., AND MASQUELIER, T. Stdp-based spiking deep convolutional neural networks for object recognition. *Neural Networks* 99 (2018), 56–67.
- [50] KOMURA, Y., TAMURA, R., UWANO, T., NISHIJO, H., KAGA, K., AND ONO, T. Retrospective and prospective coding for predicted reward in the sensory thalamus. *Nature* 412, 6846 (2001), 546.
- [51] KRIZHEVSKY, A., SUTSKEVER, I., AND HINTON, G. E. Imagenet classification with deep convolutional neural networks. In *Advances in neural information processing systems* (2012), pp. 1097–1105.
- [52] KROTOV, D., AND HOPFIELD, J. J. Unsupervised learning by competing hidden units. *Proceedings of the National Academy of Sciences* 116, 16 (2019), 7723–7731.
- [53] LAROCHELLE, H., MANDEL, M., PASCANU, R., AND BENGIO, Y. Learning algorithms for the classification restricted boltzmann machine. *Journal of Machine Learning Research* 13, Mar (2012), 643–669.
- [54] LEE, J. H., DELBRUCK, T., AND PFEIFFER, M. Training deep spiking neural networks using backpropagation. *Frontiers in neuroscience* 10 (2016), 508.
- [55] LEWANDOWSKY, S. On the relation between catastrophic interference and generalization in connectionist networks. *Journal of Biological Systems* 2, 03 (1994), 307–333.
- [56] MAASS, W. Networks of spiking neurons: the third generation of neural network models. *Neural networks* 10, 9 (1997), 1659–1671.
- [57] MACNEIL, D., AND ELIASMITH, C. Fine-tuning and the stability of recurrent neural networks. *PLOS ONE* 6, 9 (09 2011), 1–16.
- [58] MAGEE, J. C., AND JOHNSTON, D. A synaptically controlled, associative signal for hebbian plasticity in hippocampal neurons. *Science* 275, 5297 (1997), 209–213.
- [59] MCCLOSKEY, M., AND COHEN, N. J. Catastrophic interference in connectionist networks: The sequential learning problem. *The psychology of learning and motivation* 24, 109 (1989), 92.
- [60] MEIER, E., HERTZ, L., AND SCHOUSBOE, A. Neurotransmitters as developmental signals. *Neurochemistry international* 19, 1-2 (1991), 1–15.
- [61] MEROLLA, P., ARTHUR, J., AKOPYAN, F., IMAM, N., MANOHAR, R., AND MODHA, D. S. A digital neurosynaptic core using embedded crossbar memory with 45pj per spike in 45nm. In *2011 IEEE custom integrated circuits conference (CICC)* (2011), IEEE, pp. 1–4.
- [62] MEROLLA, P. A., ARTHUR, J. V., ALVAREZ-ICAZA, R., CASSIDY, A. S., SAWADA, J., AKOPYAN, F., JACKSON, B. L., IMAM, N., GUO, C., NAKAMURA, Y., ET AL. A million spiking-neuron integrated circuit with a scalable communication network and interface. *Science* 345, 6197 (2014), 668–673.
- [63] MILLER, E. K., LI, L., AND DESIMONE, R. Activity of neurons in anterior inferior temporal cortex during a short-term memory task. *Journal of Neuroscience* 13, 4 (1993), 1460–1478.
- [64] MOZAFARI, M., GANJTABESH, M., NOWZARI-DALINI, A., THORPE, S. J., AND MASQUELIER, T. Bio-inspired digit recognition using reward-modulated spike-timing-dependent plasticity in deep convolutional networks. *Pattern Recognition* 94 (2019), 87–95.
- [65] NEFTCI, E., DAS, S., PEDRONI, B., KREUTZ-DELGADO, K., AND CAUWENBERGHS, G. Event-driven contrastive divergence for spiking neuromorphic systems. *Frontiers in neuroscience* 7 (2014), 272.
- [66] NEISSER, U. *Cognitive psychology: Classic edition*. Psychology Press, 2014.
- [67] O’CONNOR, P., NEIL, D., LIU, S.-C., DELBRUCK, T., AND PFEIFFER, M. Real-time classification and sensor fusion with a spiking deep belief network. *Frontiers in neuroscience* 7 (2013), 178.
- [68] OLSHAUSEN, B. A., AND FIELD, D. J. Sparse coding with an overcomplete basis set: A strategy employed by v1? *Vision research* 37, 23 (1997), 3311–3325.

- [69] OORD, A. V. D., DIELEMAN, S., ZEN, H., SIMONYAN, K., VINYALS, O., GRAVES, A., KALCHBRENNER, N., SENIOR, A., AND KAVUKCUOGLU, K. Wavenet: A generative model for raw audio. *arXiv preprint arXiv:1609.03499* (2016).
- [70] O'REILLY, R. C. Six principles for biologically based computational models of cortical cognition. *Trends in cognitive sciences* 2, 11 (1998), 455–462.
- [71] O'REILLY, R. C., AND MUNAKATA, Y. *Computational explorations in cognitive neuroscience: Understanding the mind by simulating the brain*. MIT press, 2000.
- [72] ORORBIA, A., MALI, A., GILES, C. L., AND KIFER, D. Continual learning of recurrent neural networks by locally aligning distributed representations. *arXiv preprint arXiv:1810.07411* (2018).
- [73] ORORBIA, A., MALI, A., KIFER, D., AND GILES, C. L. Lifelong neural predictive coding: Sparsity yields less forgetting when learning cumulatively. *arXiv preprint arXiv:1905.10696* (2019).
- [74] ORORBIA, A. G., HAFFNER, P., REITTER, D., AND GILES, C. L. Learning to adapt by minimizing discrepancy. *arXiv preprint arXiv:1711.11542* (2017).
- [75] ORORBIA, A. G., AND MALI, A. Biologically motivated algorithms for propagating local target representations. In *Proceedings of the AAAI Conference on Artificial Intelligence* (2019), vol. 33, pp. 4651–4658.
- [76] ORORBIA, A. G., MALI, A., KELLY, M. A., AND REITTER, D. Like a Baby: Visually Situated Neural Language Acquisition. In *Proceedings of the 57th Annual Meeting of the Association for Computational Linguistics* (Florence, Italy, 2019).
- [77] ORORBIA, A. G., MALI, A., KIFER, D., AND GILES, C. L. Deep credit assignment by aligning local representations. *arXiv preprint arXiv:1803.01834* (2018).
- [78] ORORBIA, I., ALEXANDER, G., GILES, C. L., AND REITTER, D. Online semi-supervised learning with deep hybrid boltzmann machines and denoising autoencoders. *arXiv preprint arXiv:1511.06964* (2015).
- [79] ORORBIA II, A., GILES, C. L., AND REITTER, D. Learning a deep hybrid model for semi-supervised text classification. In *Proceedings of the 2015 Conference on Empirical Methods in Natural Language Processing* (2015), pp. 471–481.
- [80] ORORBIA II, A. G., MIKOLOV, T., AND REITTER, D. Learning simpler language models with the differential state framework. *Neural Computation* 29, 12 (2017), 3327–3352.
- [81] ORORBIA II, A. G., REITTER, D., WU, J., AND GILES, C. L. Online learning of deep hybrid architectures for semi-supervised categorization. In *Machine Learning and Knowledge Discovery in Databases (Proceedings, ECML PKDD 2015)*, vol. 9284 of *Lecture Notes in Computer Science*. Springer, Porto, Portugal, 2015, pp. 516–532.
- [82] PARK, Y., AND KELLIS, M. Deep learning for regulatory genomics. *Nature biotechnology* 33, 8 (2015), 825.
- [83] PASCANU, R., MIKOLOV, T., AND BENGIO, Y. On the difficulty of training recurrent neural networks. In *International conference on machine learning* (2013), pp. 1310–1318.
- [84] POPLIN, R., VARADARAJAN, A. V., BLUMER, K., LIU, Y., MCCONNELL, M. V., CORRADO, G. S., PENG, L., AND WEBSTER, D. R. Prediction of cardiovascular risk factors from retinal fundus photographs via deep learning. *Nature Biomedical Engineering* 2, 3 (2018), 158.
- [85] QUERLIOZ, D., BICHLER, O., DOLLFUS, P., AND GAMRAT, C. Immunity to device variations in a spiking neural network with memristive nanodevices. *IEEE Transactions on Nanotechnology* 12, 3 (2013), 288–295.
- [86] RAINER, G., RAO, S. C., AND MILLER, E. K. Prospective coding for objects in primate prefrontal cortex. *Journal of Neuroscience* 19, 13 (1999), 5493–5505.
- [87] RAJKOMAR, A., OREN, E., CHEN, K., DAI, A. M., HAJAJ, N., HARDT, M., LIU, P. J., LIU, X., MARCUS, J., SUN, M., ET AL. Scalable and accurate deep learning with electronic health records. *NPJ Digital Medicine* 1, 1 (2018), 18.
- [88] RAO, R. P., AND BALLARD, D. H. Predictive coding in the visual cortex: a functional interpretation of some extra-classical receptive-field effects. *Nature neuroscience* 2, 1 (1999).
- [89] RATCLIFF, R. Connectionist models of recognition memory: constraints imposed by learning and forgetting functions. *Psychological review* 97, 2 (1990), 285.
- [90] RUECKERT, E., KAPPEL, D., TANNEBERG, D., PECEVSKI, D., AND PETERS, J. Recurrent spiking networks solve planning tasks. *Scientific reports* 6 (2016), 21142.
- [91] SAMADI, A., LILICRAP, T. P., AND TWEED, D. B. Deep learning with dynamic spiking neurons and fixed feedback weights. *Neural computation* 29, 3 (2017), 578–602.

- [92] SUTSKEVER, I., HINTON, G. E., AND TAYLOR, G. W. The recurrent temporal restricted boltzmann machine. In *Advances in Neural Information Processing Systems* (2009), pp. 1601–1608.
- [93] SZLAM, A. D., GREGOR, K., AND CUN, Y. L. Structured sparse coding via lateral inhibition. In *Advances in Neural Information Processing Systems* (2011), pp. 1116–1124.
- [94] TAYLOR, G. W., HINTON, G. E., AND ROWEIS, S. T. Modeling human motion using binary latent variables. In *Advances in neural information processing systems* (2007), pp. 1345–1352.
- [95] THIELE, J. C., BICHLER, O., AND DUPRET, A. Event-based, timescale invariant unsupervised online deep learning with stdp. *Frontiers in computational neuroscience* 12 (2018), 46.
- [96] THRUN, S., AND MITCHELL, T. M. Lifelong robot learning. *Robotics and autonomous systems* 15, 1-2 (1995), 25–46.
- [97] WERBOS, P. J., ET AL. Backpropagation through time: what it does and how to do it. *Proceedings of the IEEE* 78, 10 (1990), 1550–1560.
- [98] WIDROW, B., AND HOFF, M. E. Adaptive switching circuits. Tech. rep., Stanford Univ Ca Stanford Electronics Labs, 1960.
- [99] WISKOTT, L., AND SEJNOWSKI, T. J. Slow feature analysis: Unsupervised learning of invariances. *Neural computation* 14, 4 (2002), 715–770.
- [100] XIAO, H., RASUL, K., AND VOLLGRAF, R. Fashion-mnist: a novel image dataset for benchmarking machine learning algorithms. *arXiv preprint arXiv:1708.07747* (2017).
- [101] ZENG, G., CHEN, Y., CUI, B., AND YU, S. Continual learning of context-dependent processing in neural networks. *Nature Machine Intelligence* 1, 8 (2019), 364–372.
- [102] ZHAO, B., DING, R., CHEN, S., LINARES-BARRANCO, B., AND TANG, H. Feedforward categorization on aer motion events using cortex-like features in a spiking neural network. *IEEE transactions on neural networks and learning systems* 26, 9 (2014), 1963–1978.
- [103] ZMARZ, P., AND KELLER, G. B. Mismatch receptive fields in mouse visual cortex. *Neuron* 92, 4 (2016), 766–772.

Appendix

Algorithmic Specification

In this section, we present the full pseudocode, i.e., Algorithm 1, for computing state updates and synaptic weight updates for an L -layered spiking neural coding network (SpNCN) at any point in continuous time. Note that additional coefficients/hyper-parameters are input to the SpNCN’s routines, i.e., $\{\gamma_j, \kappa, \alpha_j, \beta\}$, and are values set by the user at the start of simulation (meaning of each is described in the main paper). The pseudocode presented below demonstrates the operation of a general SpNCN that could use any kind of spike response model (SRM), so long as the SRM can make use of the variable $\mathbf{J}^\ell(t)$ (current) in the form developed in this paper. Possible choices for the SRM could be a variation of the leaky integrate-and-fire (LIF) model, the Hodgkin–Huxley [42] model, or the Izhikevich [46] model.

Algorithm 1 Process for running inference and evolving weights in the SpNCN.

```

1: Inputs:  $\mathbf{x}_n, \mathbf{y}_n, \Theta = \{W_1, E_1, \dots, W_L, E_L\}, \Upsilon = \{\mathbf{J}^1(t), \dots, \mathbf{J}^L(t)\}, \mathcal{E} = \{\mathbf{e}^1(t), \dots, \mathbf{e}^L(t)\},$ 
2:    $\mathcal{V} = \{\mathbf{v}^1(t), \dots, \mathbf{v}^L(t)\}, \mathcal{S} = \{\mathbf{s}^1(t), \dots, \mathbf{s}^L(t)\}, \mathcal{Z} = \{\mathbf{z}^1, \dots, \mathbf{z}^L\}$ 
3: function COMPUTESTATES( $\mathbf{x}, \mathbf{y}, \Theta, \Upsilon, \mathcal{E}, \mathcal{V}, \mathcal{Z}, \gamma_j, \kappa, \alpha_f$ ) ▷ Compute variable state updates
4:   for  $\ell = 1$  to  $L$  do
5:     // Extract current layer-wise variable states
6:      $\mathbf{J}^\ell(t) \leftarrow \Upsilon[\ell], \mathbf{v}^\ell(t) \leftarrow \mathcal{V}[\ell], \mathbf{z}^\ell(t) \leftarrow \mathcal{Z}[\ell], \mathbf{e}^\ell(t) \leftarrow \mathcal{E}[\ell], \mathbf{e}^{\ell-1}(t) \leftarrow \mathcal{E}[\ell-1]$ 
7:     // Update values of currents
8:     if  $\ell < L$  then
9:        $\mathbf{J}^\ell(t) = (1 - \kappa)\mathbf{J}^\ell(t) + \kappa \left( -\gamma_j \mathbf{J}^\ell(t) + \phi(-\mathbf{e}^\ell(t) + E^\ell \cdot \mathbf{e}^{\ell-1}(t)) \right)$ 
10:    else
11:       $\mathbf{J}^\ell(t) = (1 - \kappa)\mathbf{J}^\ell(t) + \kappa \left( -\gamma_j \mathbf{J}^\ell(t) + \phi(E^\ell \cdot \mathbf{e}^{\ell-1}(t)) \right)$ 
12:      // Compute voltage and spike values given a chosen SRM, apply filter to spike variable
13:       $(\mathbf{v}^\ell(t), \mathbf{s}^\ell(t)) \leftarrow f_{srn}(\mathbf{v}^\ell(t), \mathbf{J}^\ell(t)), \quad \mathbf{z}^\ell(t) = (\alpha_f \mathbf{z}^\ell(t)) \otimes (1 - \mathbf{s}^\ell(t)) + \mathbf{s}^\ell(t)$ 
14:      // Make top-down predictions & compute error neurons
15:      for  $\ell = L$  to  $1$  do
16:         $\mathbf{z}_\mu^\ell = W^\ell \cdot \mathbf{s}^\ell(t), \quad \mathbf{e}^\ell(t) = (\mathbf{z}_\mu^\ell - \mathbf{z}^\ell(t))$ 
17:      return  $\Upsilon, \mathcal{E}, \mathcal{V}, \mathcal{S}$  ▷ Return overwritten/updated variables
18: function COMPUTEUPDATES( $\mathcal{S}, \mathcal{E}, \beta$ ) ▷ Compute parameter adjustments
19:   for  $\ell = 1$  to  $L$  do
20:      $\mathbf{s}^\ell(t) \leftarrow \mathcal{S}[\ell], \mathbf{e}^{\ell-1}(t) \leftarrow \mathcal{E}[\ell-1]$  ▷ Extract relevant layer-wise statistics
21:      $\Delta W^\ell = \mathbf{e}^{\ell-1}(t) \cdot (\mathbf{s}^\ell(t))^T, \quad \Delta E^\ell = -\beta (\mathbf{s}^\ell(t) \cdot (\mathbf{e}^{\ell-1}(t))^T)$ 
22:   return  $\Delta = \{\Delta W_1, \Delta E_1, \dots, \Delta W_L, \Delta E_L\}$  ▷ Return updates

```

The X-O Pattern Classification Task

As a sanity check, we originally started by evaluating our proposed SpNCN on a simple pattern recognition task often used in evaluating the basic discriminative ability of SNNs in general [15]. The task consists of simply distinguishing between a circle (“O”) shape from an X-cross (“X”) binary pattern. The image patterns are 16×16 (binary) pixel grids, with backgrounds that are black (pixel value of 0) and foreground elements that are white (pixel value of 255).

Training the model consisted of presenting a sequence of X and O patterns for a fixed duration of time, i.e., $T_{st} = 60$ ms and $T_{ist} = 30$ ms (which is simulated by clamping the error neurons at the sensory/input layer to zero vectors within this inter-stimulus interval, allowing the internal neurons to reach their resting potential). After a brief training period of presenting a few patterns, the SpNCN is evaluated on the following test sequence: $\{O, O, X, X, O, X, X, X, X, O, O, X, O\}$, where each pattern also presented for a stimulus time of $T_{st} = 100$ ms. After presenting only a few of these toy patterns to the network, the SpNCN was able to reach 100% mean accuracy on the test sequence above (averaged over 10 trials).

Derivative-Free Broadcast Feedback Alignment (df-BFA)

In this paper, we train a spiking neural network (SNN) with broadcast feedback alignment (BFA), much as was done in [91]. For direct comparability to our proposed spike-triggered local representation alignment for training systems of

spiking neurons without derivatives, we specifically implemented and compared to a derivative-free variant of BFA (df-BFA). Focusing on this algorithm allows us to work with spike response models (SRMs) of any kind directly (such as the leaky integrate-and-fire, LIF, model of this paper and others). Furthermore, this algorithm does not require continuous approximations of activities, much as was needed in [91]. This makes SNNs trained with BFA comparable to the spiking neural coding networks (SpNCNs) of this paper, and furthermore, more general.

Specifically, our implementation of *df-BFA* was as follows, which we will describe using the same notation developed in this paper (which also makes it consistent with the machine learning research related to the general neural coding network [74, 72, 73]). The input current to any internal layer ℓ of a feedforward SNN trained by *df-BFA*, is expressed as:

$$\mathbf{J}^\ell(t) = (1 - \kappa)\mathbf{J}^\ell(t) + \kappa \left(-\gamma\mathbf{J}^\ell(t) + \phi(W^\ell \cdot \mathbf{s}^{\ell-1}(t)) \right) \quad (11)$$

which is then provided to the desired SRM, $(\mathbf{v}^\ell(t), \mathbf{s}^\ell(t)) \leftarrow f_{srms}(\mathbf{v}^\ell(t), \mathbf{J}^\ell(t))$. γ controls the strength of the conductance leak, $\phi(\cdot)$ is a nonlinearity applied to the incoming signal pool (in this work, $\phi(v) = v$), and κ is the conductance time constant. In this paper, we use the same LIF SRM used within the SpNCN. To generate the necessary learning signals under *df-BFA*, we introduce fixed, randomly initialized feedback (alignment) weights F^ℓ that directly connect the error neurons found at the output of the network to each layer within the SNN. The top (L) layer $\hat{\mathbf{y}}(t) = \text{softmax}(W^L \cdot \mathbf{s}^{L-1}(t))$ of the SNN network is simply a softmax predictor (or a soft lateral competition layer where a winner-take-all scheme is used to get the class prediction), where $\hat{\mathbf{y}}(t)$ is the model’s current prediction for \mathbf{y} . The output error neurons are modeled by the equation $\mathbf{e}^L(t) = (\hat{\mathbf{y}}(t) - \mathbf{y})$ noting that, much like in [91], these error neurons could be made to be made more biologically-realistic by creating two separate populations where one transmits via excitatory synapses and the other via inhibitory synapses. The update for the weights of layer ℓ is then:

$$\Delta W^\ell = \mathbf{d}^\ell \cdot (\mathbf{s}^{\ell-1})^T, \text{ where, } \mathbf{d}^\ell = \phi_e(F^\ell \cdot \mathbf{e}^L(t)). \quad (12)$$

Note that the top-layer/prediction weights do not use the above equation, since they connect directly to the output units, and use an update calculated as: $\Delta W^L = \mathbf{e}^L \cdot (\mathbf{s}^{L-1})^T$. We extend the original BFA approach by incorporating what we call an “error function”, $\phi_e(\cdot)$, which is an element-wise nonlinearity applied to the teaching signal vector(s). We found in our experiments that using this function improved the stability of BFA. We set $\phi_e(v) = \text{sign}(v)$, or the signum function.

Surprisingly, the *df-BFA* scheme works quite well and, in our preliminary experiments, appeared to be reasonably robust to the initialization of the feedback weights F^ℓ (which are held fixed during learning). As a result, this simple synaptic update rule allows us to train SNNs of the same depth as the SpNCNs trained in this paper, yielding a strong baseline.

Derivative-Free Direct Random Target Propagation (df-DRTP)

As another interesting baseline, we further implement the very recently proposed direct random target propagation algorithm and extend it by omitting its dependence on the activation function’s first derivative so that way we may directly apply it to the same SNN architecture as we do for df-BFA. The underlying neural architecture is the same SNN as described in the section for BFA.

Under df-DRTP, which introduces fixed random projection synaptic matrices P^ℓ , the updates for the weights of layer ℓ are as simply as follows:

$$\Delta W^\ell = \mathbf{d}^\ell \cdot (\mathbf{s}^{\ell-1})^T, \text{ where, } \mathbf{d}^\ell = \phi_e(P^\ell \cdot \mathbf{y}) \quad (13)$$

where we see that now the updates to the layerwise synapses are local in nature given that we now randomly project (with fixed initial values) the actual target label vector \mathbf{y} to create a proxy training signal for any particular layer ℓ . Note that $\phi_e(v) = \text{sign}(v)$, just as was done for BFA described earlier.